

RESEARCH

Open Access



Effects of mesenchymal stem cells from different sources on the biological functions of multiple myeloma cells

Yanju Li^{1†}, Yang Liu^{2†}, Xu Yang^{2†}, Bo Yang², Jinyang Cheng², Juan Chen², Xiaoshuang Yuan¹, Xiao Xu³, Guanyang Liu¹, Zhixu He^{4*} and Feiqing Wang^{2,5*} 

Abstract

Background The therapeutic benefits of mesenchymal stromal cells (MSCs) are largely dependent on paracrine factors, but the supernatants of the different MSCs may have different effects on multiple myeloma (MM) cells. Therefore, this study compared supernatants of bone marrow-derived mesenchymal stromal cells (BM-MSCs) with umbilical cord wharton's jelly's mesenchymal stem cells (UC-WJ MSCs) in different states (non-senescent and replicative senescence) on the MM cells.

Methods We extracted human BM-MSCs and UC-WJ MSCs in vitro and used H₂O₂ to induce replicative senescence. Concentrated supernatants from MSCs and senescent MSCs (SMSCs) were added to MM cells. Cell proliferation, the cell cycle, apoptosis, cell migration, tumor stemness factor expression, and cytokine expression levels were analyzed. Transcription regulation of signaling pathways was discussed.

Results We successfully isolated and identified BM-MSCs, UC-WJ MSCs, and SMSCs. When concentrated supernatants from BM-MSCs, UC-WJ MSCs, senescent BM-MSCs (SBM-MSCs), senescent UCWJ MSCs (SUC-WJ MSCs) were used to treat MM cells, BMMSCs and SBM-MSCs supernatants promoted the proliferation of MM cells, with a more pronounced effect by SBM-MSCs. UC-WJ MSCs and SUC-WJ MSCs supernatants inhibited the viability and proliferation of MM cells. BM-MSCs and SBM-MSCs supernatants increased the proportion of MM cells in the S-phase, with the effect of SBM-MSCs being more evident. UC-WJ MSCs and SUC-WJ MSCs supernatants arrested MM cells in the G0/G1 phase. BM-MSCs and SBM-MSCs supernatants enhanced the migration and tumor stemness of MM cells, with SBMMSCs having a more dramatic effect. UC-WJ MSCs and SUC-WJ MSCs supernatants inhibited the migration and tumor stemness of MM cells, with UC-WJ MSCs having a more inhibitory effect. IL-6 and VEGFA expression correlated negatively with the survival of patients with MM according to online database analysis, in addition, we found that the expression of IL-6 and VEGFA was higher in MM patients through GEO database analysis. BM-MSCs and SBM-MSCs supernatants treatment increased the expression of IL-6 and VEGFA on MM cells, while UC-WJ MSCs and SUC-WJ MSCs

[†]Yanju Li, Yang Liu and Xu Yang contributed equally to this work.

*Correspondence:
Zhixu He
hzxgzy@163.com
Feiqing Wang
wfq8806@163.com

Full list of author information is available at the end of the article



supernatants inhibited their expression. Signal pathway validation showed that the biological function of MSCs in MM is closely related to the PI3K/AKT/NF- κ B pathway.

Conclusion The supernatants of BM-MSCs promote the proliferation of MM cells, On the contrary, the supernatants of UC-WJ MSCs inhibit MM cell proliferation. We observed that MSCs from different sources and different states have contrasting biological functions in MM cells. Furthermore, this research was provided to the optimal cancer gene therapy vector for MM was UC-WJ MSCs, even UC-WJ MSCs was in the state of senescence.

Keywords Mesenchymal stem cells, Senescence, Multiple myeloma, Biological functions, PI3K/AKT/NF- κ B

Introduction

Multi-tumor model studies have shown that MSCs delivered via vein or artery have a preference for tumor sites, mainly due to factors secreted by tumor cells and/or inflammatory mediators produced by damaged tissues [1, 2], so some reports have suggested that MSCs can be used as vectors for cancer gene therapy [3, 4]. However, MSCs of distinct origins have different biological functions and therapeutic effects, with a dual role in stimulating growth or inhibiting progression in cancer [5]. Experiments have shown that extracellular vesicles from BM-MSCs can promote the malignant progression of MM [6]. BM-MSCs could promote MM cell clone formation and proliferation, whereas umbilical cord mesenchymal stem cells (UC-MSCs) significantly inhibited MM cell clonality and proliferation in vitro and inhibited the subcutaneous tumor growth in mice in vivo [7]. These studies suggested a close interaction between MM cells and BM-MSCs and UC-MSCs were different, however, the underlying mechanisms are not fully understood.

Previous studies have found that in the microenvironment of multiple myeloma, abnormally proliferated plasma cells have acclimated mesenchymal stem cells into senescence [8, 9]. Senescent MSCs usually have the unique property of secreting large quantities of chemokines and cytokines, termed the senescence-associated secretory phenotype (SASP). SASP triggering the inception of deadly degenerative diseases by paracrine factors, such as cancer [10]. Therefore, in the present study, we explored the effect of supernatants of BM-MSCs and UC-WJ MSCs and their senescent populations on MM. Furthermore, to provide the optimal cancer gene therapy vector for MM patients.

Methods

Cell lines and culture

MM cell lines (RPMI8226 and U266) [11, 12] were cultured in Roswell Park Memorial Institute (RPMI) 1640 medium containing 10% fetal bovine serum (FBS) and 1% penicillinstreptomycin. BM-MSCs and UC-WJ MSCs were grown in L-Dulbecco's modified Eagle's medium (L-DMEM) supplemented with 10% FBS and 1% penicillinstreptomycin.

Isolation of human BM-MSCs and UC-WJ MSCs

Human BM-MSCs were purified using Ficoll density gradient centrifugation and the adherent method. Cells at 3~5 generation were selected for the experiments, and their immunophenotypes were identified using flow cytometry.

UC-WJ MSCs were extracted using the tissue block adhesion method. The umbilical cord tissue was washed twice with phosphate buffered saline (PBS) and thoroughly cleaned to remove any blockages. After cleaning and disinfecting with ethanol, the umbilical vein was removed and the umbilical cord was cut into small pieces (about 1 cm long) and evenly spread in a 100 mm² petri dish. Then, L-DMEM complete medium containing 10% FBS was added to the wall after attachment, and the dish was placed in a 5% CO₂ incubator at 37 °C for primary culture. We exchanged the medium every 3 days, and when the cells reached 80% confluence, they were passaged. The immunophenotypes of the cells at 3~5 generation were identified using flow cytometry.

Osteogenesis lipid induction experiment

Third generation UC-WJ MSCs and BM-MSCs in good condition were trypsin digested and seeded in a labeled 6-well plate at a density of 2×10^4 cells/well. When the cells reached about 40% confluence, the medium was replaced with 2 mL of osteogenic induction medium (DMEM medium containing 10% FBS, 0.1 μ mol/L dexamethasone, 10 mmol/L β glycerophosphate, 50 mg/L vitamin C, 100 mg/L penicillin, and 100 U/mL streptomycin). Alizarin red staining was performed on the 14th day. The cells were fixed for 30 min using 40 g/L paraformaldehyde, washed thrice using PBS, and stained using 2% alizarin red S for 20 min at room temperature. The formation of mineralized nodules was observed under an optical microscope.

Healthy UC-WJ MSCs and BM-MSCs from passage 3 were seeded in 6-well plates at a density of 2×10^4 cells/well, and grown until they reached 100% confluence. The medium was replaced with 2 mL of adipogenic induction medium (DMEM medium containing 10% fetal bovine serum, 1 μ mol/L dexamethasone, 60 μ mol/L indomethacin, 0.5 mmol/L 1-methyl-3-isobutylxanthine, 100 mg/L penicillin, and 100 U/mL streptomycin). The adipogenic

induction medium was replaced every 3 days. Oil red O staining was performed on the 14th day. The induced cells were fixed for 30 min using 40 g/L paraformaldehyde, washed thrice using PBS, and then stained using oil red O staining solution for 30 min at room temperature. An optical microscope was used to observe the stained cells.

Inducing cell senescence

To induce cellular senescence, MSCs were subjected to hydrogen peroxide (H₂O₂) oxidative stress. Semi-confluent cells were exposed to 200 μM H₂O₂ for 2 h. Thereafter, the cells rinsed using PBS and grown for 3 days in fresh medium. To evaluate cell senescence, according to the manufacturer's instructions, we carried out a βgalactosidase assay using a senescence-associated β-galactosidase staining kit (SABGal; Beyotime, Jiangsu, China). In each group (*n* = 3), senescent cells were viewed using an optical microscope and images were obtained from three random fields.

Collection of concentrated supernatants of MSCs

The different MSCs (BM-MSCs, UC-WJ MSCs), senescent BM-MSCs (SBM-MSCs), and senescent UC-WJ MSCs (SUC-WJ MSCs) were inoculated into 100 mm² dishes at 1 × 10⁶ cells. After the cells reached approximately 80% confluence, the medium was replaced with serum-free L-DMEM, and after 48 h, we collected the supernatant by centrifugation at 4 °C for 60 min at centrifugal force 5300×g using a truncated 100 kDa ultra-filtration tube. The collected concentrated solution was filtered and stored at -80 °C.

3-(4,5-dimethylthiazol-2-yl)-2,5-diphenyltetrazolium bromide (MTT) assay to evaluate cell viability

RPMI8226 and U266 cells were seeded into 96-well plates at 100 μL/well (1 × 10⁴ cells/ml) and incubated at 37 °C overnight in a 5% CO₂ humidified incubator. Thereafter, the cells were then pretreated with various concentrated supernatants of MSCs (BM-MSCs, UCMSCs, SBM-MSCs, SUC-WJ MSCs) for 1, 2, 3, 4, 5, 6, and 7 days. Then, MTT solution (20 μL) was added to each well, followed by incubation for 4 h at 37 °C with 5% CO₂. Finally, a microplate reader was used to determine the absorbance at 570 nm.

Cell apoptosis analysis using flow cytometry

Healthy RPMI8226 and U266 cells were inoculated into sterile 25 cm² culture flasks at 1 × 10⁵ cells/bottle and grown in a CO₂ atmosphere for 12 h. After synchronization, different MSCs concentrated supernatants (BM-MSCs, UC-WJ MSCs, SBM-MSCs, and SUC-WJ MSCs) were added to the medium and culture was continued for 48 h. The cells were collected by centrifugation (5 min

at 1000 rpm). The supernatant was removed, the cells were resuspended in 500 μL of PBS, and then added with Annexin V-fluorescein isothiocyanate (FITC) (5 μL) and propidium iodide (PI) (5 μL), mixed, and reacted at room temperature for 15 min in the dark.

Cell cycle analysis using flow cytometry

Healthy RPMI8226 and U266 cells were inoculated into sterile 25 cm² culture flasks at 1 × 10⁵ cells/bottle and grown in a CO₂ atmosphere for 12 h. After synchronization, different MSCs concentrated supernatants (BM-MSCs, UC-WJ MSCs, SBM-MSCs, and SUC-WJ MSCs) were added to the medium and cultured was continued for 48 h. The cells were collected by centrifugation (3100 g, 5 min), washed using pre-cooled PBS, centrifuged again, and resuspended in pre-cooled PBS. Pre-cooled 70% ethanol was added to the suspension, which was incubated overnight at 4 °C for fixation. Next day, the fixed cells were centrifuged and the cell pellet was washed twice using PBS. Then, RNase A (50 μL) and PI (450 μL) were added and the cells were incubated for 30 min at 4 °C. Finally, flow cytometry was used to analyze the cell cycle (BD C6 Plus Cell Analyzer). The results were analyzed using FlowJo 10.0 software (Tree Star Inc., Ashland, OR, USA).

Transwell invasion assay

Analysis of cell migration and invasion capacity was carried out using transwell assays. We added 1 × 10⁵ cells (200 μL) into the upper chamber of the transwell cassette (8 μm, Corning Inc., Corning, NY, USA) and different MSCs concentrated supernatants (BM-MSCs, UC-WJ MSCs, SBM-MSCs, and SUC-WJ MSCs) were added according to the experimental requirements. We added 600 μL of RPMI-1640 medium with 20% FBS to the lower chamber. After 48 h, the cells remaining in the upper chamber were wiped off, and 10 μL of 10 mg/ml MTT were added to each well and incubated at 37 °C for 4 h. We removed the supernatant, added 150 μL of dimethyl sulfoxide (DMSO), and the reaction was allowed to proceed for 15~20 min. Thereafter, a microplate reader was used to determine the OD values at 570 nm.

Western blotting analysis

Radioimmunoprecipitation (RIPA) lysis buffer containing phenylmethylsulfonyl fluoride (PMSF), phosphatase inhibitors, and protease inhibitors, was used to extract total proteins from cells. Sodium dodecyl sulfate-polyacrylamide gel electrophoresis (SDS-PAGE; 6–12%) (Solarbio, Beijing, China) was used to separate equal amounts of protein, which were then transferred electrophoretically to polyvinylidene fluoride (PVDF) membranes (0.45 μM, Millipore, Billerica, MA, USA). 5% skim milk was used to block the membranes

at room temperature for 1 h. The membranes were then incubated gently overnight at 4 °C with the following primary antibodies: anti-phosphorylated protein 53 (P53), antiglyceraldehyde-3-phosphate dehydrogenase (GAPDH), anti-cyclin dependent kinase inhibitor 1 A (p21), anti-nuclear factor kappa B (NF- κ B), antiphosphatidylinositol-4,5-bisphosphate 3-kinase (PI3K), anti-phosphorylated (P)PI3K, anti-protein kinase B (AKT), antiPAKT (1:1,000; Beyotime), anti-cyclin dependent kinase 6 (CDK6), antiCyclinE1, anti-SRY-box transcription factor 2 (SOX2), anti-NANOG, anti-octamer-binding protein 4 (OCT4) (1:1,000; ProteinTech, Rosemont, IL, USA), anti-Vascular endothelial growth factor A (VEGFA), anti-interleukin-6 (IL6), anti-E-Cadherin and anti-N-Cadherin (1:1,000; Cell Signaling Technology, Danvers, MA, USA). The membranes were washed thrice using Tri-buffered saline Tween 20 (TBST, Solarbio) and then incubated with goat anti-rabbit and goat anti-mouse horseradish peroxidase (HRP)-linked secondary antibodies 1:5000 (Boster, Wuhan, China) at room temperature for 2 h. Finally, the immunoreactive protein bands were detected using ultra-sensitive ECL chemiluminescence (Boster). Image J software (NIH, Bethesda, MD, USA) was used to quantify the grey values of the protein bands, normalized to that of GAPDH.

Functional exploration of differentially expressed genes from MM

The PrognScan database (<http://dna00.bio.kyutech.ac.jp/PrognScan/>) was utilized to aggregate all available datasets, providing a convenient and reliable method for investigating the prognostic significance of genes. We employed the PrognScan GSE2658 of database data to assess the prognostic relevance of core target molecules across MM, the endpoint was disease specific survival. The threshold for inclusion in further analysis was established as p corrected < 0.05.

The gene expression analysis dataset GSE6477 was downloaded from the GEO database <http://www.ncbi.nlm.nih.gov/geo/>, and included 149 MM patient samples and 13 healthy subjects as training datasets. The expression difference between IL-6 and VEGFA was analyzed using R.4.3.2 language.

Statistical analysis

All data are shown as the mean \pm standard deviation (SD). Statistical analysis was performed using GraphPad Prism software (GraphPad Software, San Diego, CA, USA). Differences between or among groups were analyzed using Student's t -test or one-way analysis of variance (ANOVA). Statistical significance was indicated by P values less than 0.05.

Results

Extraction and identification of MSCs

We isolated MSCs from bone marrow and umbilical cord, and characterized their phenotype using flow cytometry. Subsequently, we assessed their differentiation potential into osteocytes and adipocytes (Figs. 1 and 2A). After 7 days of primary UC-WJ MSCs culture, a small number of cells emerged from the umbilical cord tissue, as observed under an inverted optical microscope. On the 9th day, the cells grew into colonies and formed dense structures resembling whirlpools. After digestion and subculture, the 3rd generation of UC-WJ MSCs grew with a spindle shape. On the third day of primary culture of BM-MSCs, a large number of suspended round cells could be seen under the microscope, and long spindle-shaped and triangular adherent cells could be seen at the bottom of the petri dish. After digestion and passage, round and long spindle-shaped adherent cells could be seen in passage 1 (P1) cells, and dense growth of spiral cells could be seen in P3 cells (Fig. 2B). Flow cytometry showed high expression of CD90, CD105, and CD73 in 3rd generation UC-WJ MSCs and BM-MSCs (Positive rate > 95%), and low expression of CD14, CD34, CD11b, CD45, and HLA-DR (Positive rate < 1%) (Fig. 2C). After 14 days of induction differentiation of UC-WJ MSCs and BM-MSCs in lipogenic osteogenic medium, oil red O staining showed round lipid droplets in the differentiated cells identifying them as differentiated adipocytes and orange calcium nodules were formed after alizarin red staining. Both cell populations had the ability to differentiate into bone cells and adipocytes (Fig. 2D). Thus, the isolated cells were identified as MSCs.

Identification of senescent MSCs

We used H₂O₂ to induce MSCs to senescence and identified them by flow cytometry and western blot (Fig. 3A). BM-MSCs and UC-WJ MSCs showed a fibroblast-like morphology, and after H₂O₂ induced senescence, the MSCs appeared longer and larger, and accumulated granular cytoplasmic inclusions. In aging MSCs, the percentage of cells that were stained positively with SA- β -Ga increased significantly (Fig. 3B). Flow cytometry showed that the proportion of senescent MSCs (SMSCs) in the G0/G1 phase was significantly increased, while the proportion of cells in the S-phase was significantly decreased (Fig. 3C). In SMSCs, increased age resulted in enhanced levels of p53 and p21, as assessed using western blotting (Fig. 3D).

Effect of MSCs on myeloma cell proliferation

The MTT assay was employed to assess the proliferation of multiple myeloma cells following the addition of various concentrations of MSCs (Fig. 4A). To determine the effects of UC-WJ MSCs and BM-MSCs on MM cells,

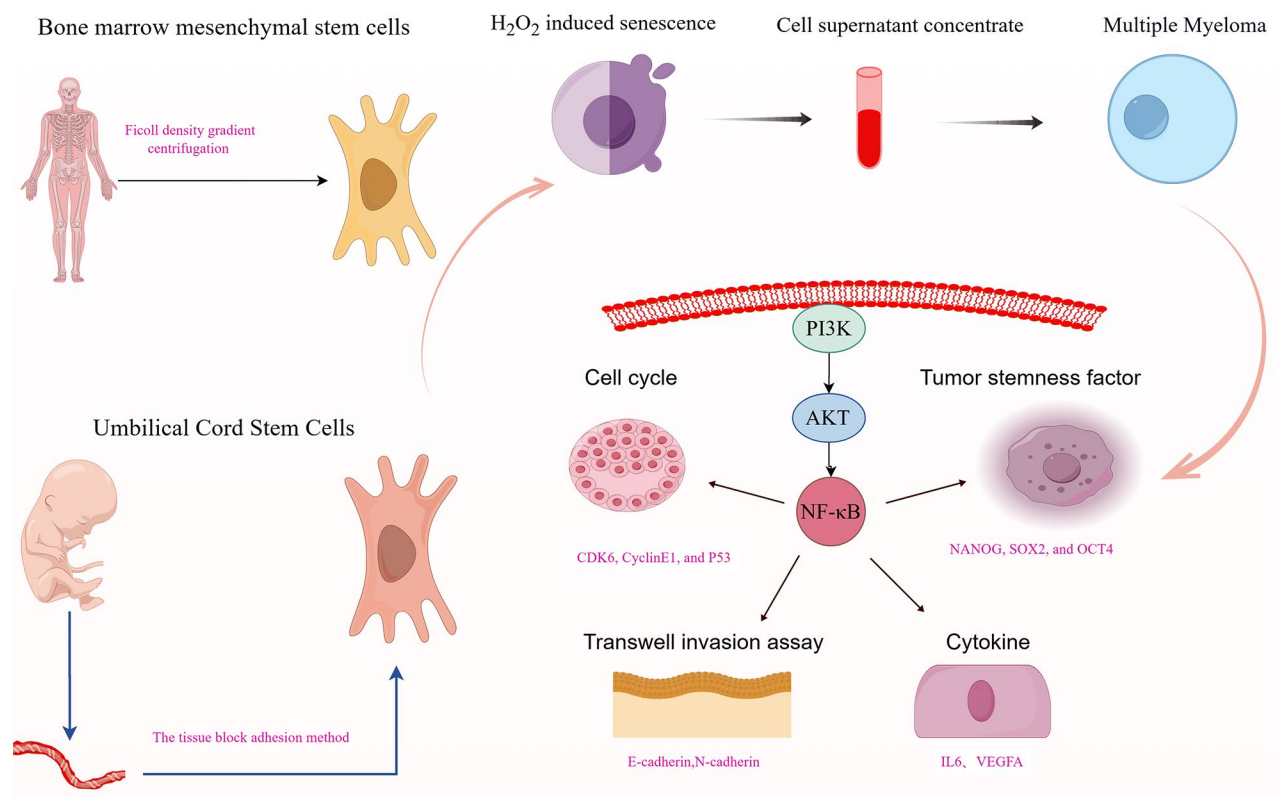


Fig. 1 Schema of experiment design: Effects of mesenchymal stem cells from different sources on the biological functions of multiple myeloma cells. Bone marrow and umbilical cord mesenchymal stem cells were extracted, and senescence induced by H_2O_2 was exerted on multiple myeloma cells in various states to observe the effects of the supernatant on the biological function of multiple myeloma cells

RPMI8226 and U266 cells were cultured with concentrated supernatants from BM-MSCs, UCMSCs, and SMSCs for 48 h. As shown in Fig. 4B, BM-MSCs and senescent BMMSCs (SBM-MSCs) supernatants promoted the proliferation of RPMI8226 and U266 cells, with the SBM-MSCs supernatant having a more significant promotion effect. UCMSCs and senescent UC-WJ MSCs (SUC-WJ MSCs) supernatants inhibited the proliferation of RPMI8226 and U266 compared with that of the blank group, and the inhibitory effect of the UC-WJ MSCs supernatant was more pronounced (Fig. 4C).

Effect of MSCs concentrated supernatants on MM cell apoptosis

Flow cytometry of different MSCs concentrates added to MM cells (Fig. 5A). To determine if UC-WJ MSCs and SUC-WJ MSCs have a pro-apoptotic effect on MM cells, MM cells (RPMI8226 and U266) were cultured with UC-WJ MSCs and SUC-WJ MSCs concentrated supernatants for 48 h, after which apoptosis was determined using flow cytometry. The early and late apoptosis rates were increased in both groups of cells, and the promotion of apoptosis was more pronounced in the cells treated with the concentrated supernatant from younger

UC-WJ MSCs (Fig. 5B); however, the differences were not statistically significant (Fig. 5C).

The influence of different MSCs on the MM cell cycle

The concentrated supernatants of BM-MSCs and SBM-MSCs were used to treat MM cells (RPMI8226 and U266) for 48 h. Flow cytometry analysis of the cell cycle showed that the BM-MSCs and SBM-MSCs supernatants increased the percentage of MM cells in the S-phase, with a larger increase in the cells treated with SBM-MSC supernatant. By contrast, UC-WJ MSCs and SUC-WJ MSCs supernatants increased the proportion of MM cells in the G0/G1 phase, with a larger increase in the cells treated with SUC-WJ MSCs supernatant (Fig. 6A). In addition, the levels of CDK6, CyclinE1, and P53 in each group were detected using western blotting. We observed that UCMSCs and SUC-WJ MSCs supernatants decreased the levels of CDK6 and CyclinE1 and increased the level of P53 in RPMI8226 and U266 cells, with the UC-WJ MSCs supernatant having a larger effect than the SUC-WJ MSCs supernatant (Fig. 6B). The BM-MSCs and SBM-MSCs supernatants increased the levels of CDK6 and CyclinE1, but reduced the levels of p53, with the BM-MSCs supernatant having a larger effect

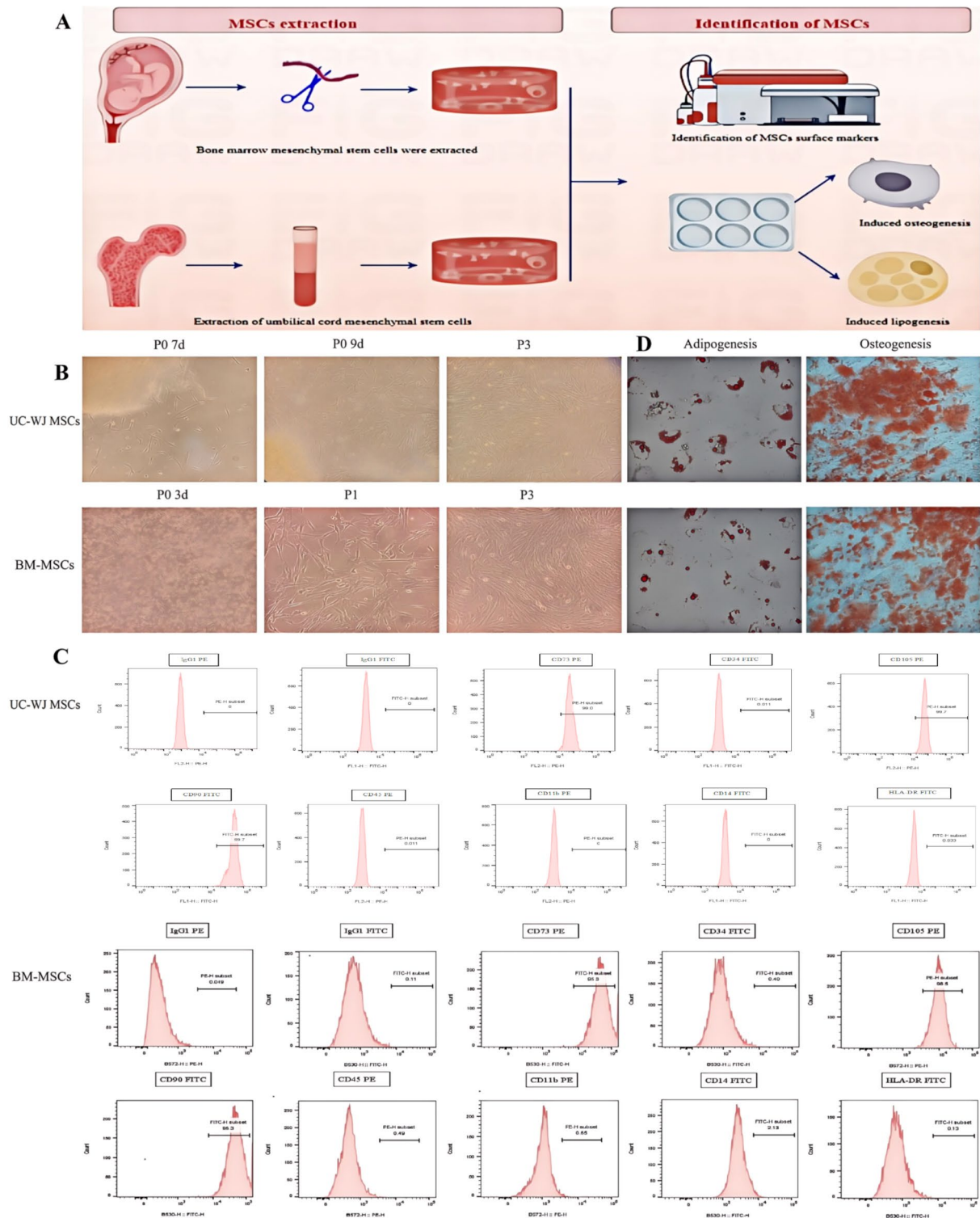


Fig. 2 Extraction and identification of MSCs. **(A)** Schema of experiment design: MSCs extraction and identification of MSCs. **(B)** Extraction and culture of BM-MSCs and UC-WJ MSCs. **(C)** MSCs phenotypes were identified by flow cytometry. **(D)** The ability of BM-MSCs and UC-WJ MSCs to differentiate into osteocytes and adipocytes

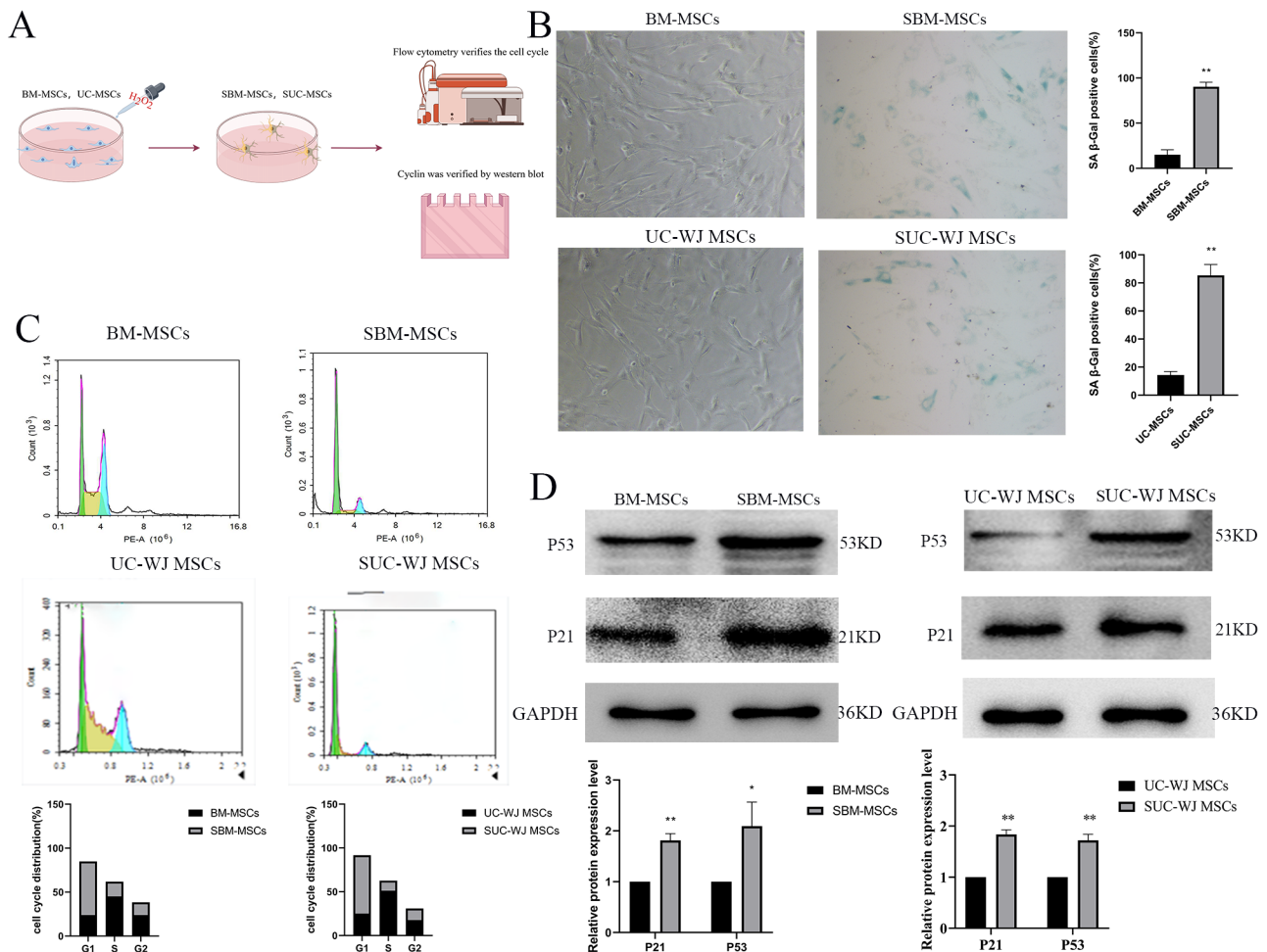


Fig. 3 Identification of MSCs. **(A)** Schema of experiment design: MSCs induced senescence and identification. **(B)** SA-β-Gal staining of senescent and non-senescent MSCs. **(C)** Flow cytometry of senescent MSCs and non-senescent MSCs. **(D)** Levels of p21 and p53 protein in senescent MSCs and non-senescent MSCs. * $P < 0.05$, ** $P < 0.01$ comparison with the control group. Full-length gels/blots are shown in Figure S1 in the Supplementary material

than the SBM-MSCs supernatant (Fig. 6B). Detection of intracellular cycle changes after addition of different MSCs concentrates to MM cells using flow cytometry (Fig. 6C).

Different MSCs affected MM cells migration in different ways

When different stem cell concentrate solutions were added to MM cells, we conducted invasion experiment (Fig. 7A). Compared with the control group, treatment of RPMI8226 and U266 cells with UC-WJ MSCs and SUC-WJ MSCs supernatants significantly inhibited their migration, and the inhibitory effect of the UC-WJ MSCs supernatant was more obvious (Fig. 7B). RPMI8226 and U266 cells migration was promoted by BMSCs and SBM-MSCs supernatants. BM-MSCs and SBM-MSCs supernatants also increased the levels of epithelial-mesenchyme transition (EMT) related proteins in RPMI8226 and U266 cells, whereas UC-WJ MSCs and SUCMSCs

supernatants decreased the levels of EMT-related proteins in RPMI8226 and U266 cells (Fig. 7C). Moreover, the promoting effect of the SBM-MSCs supernatant was more obvious (Fig. 7C).

Effect of MSCs on the levels of tumor stem cell factors in MM cells

The effects of the different concentrated supernatants of MSCs on tumor stem cell factor protein levels in MM cells (RPMI8226 and U266) were examined using western blotting. In comparison with the control group, the UC-WJ MSCs and SUC-WJ MSCs supernatants decreased the levels of tumor stem cell factors NANOG, SOX2, and OCT4 proteins, with the UCMSCs supernatant having a greater inhibitory effect than the SUC-WJ MSCs supernatant. In contrast, the BM-MSCs and SBM-MSCs supernatants increased the levels of the tumor stem cell factors NANOG, SOX2, and OCT4, with the SBM-MSCs supernatant having a greater effect than

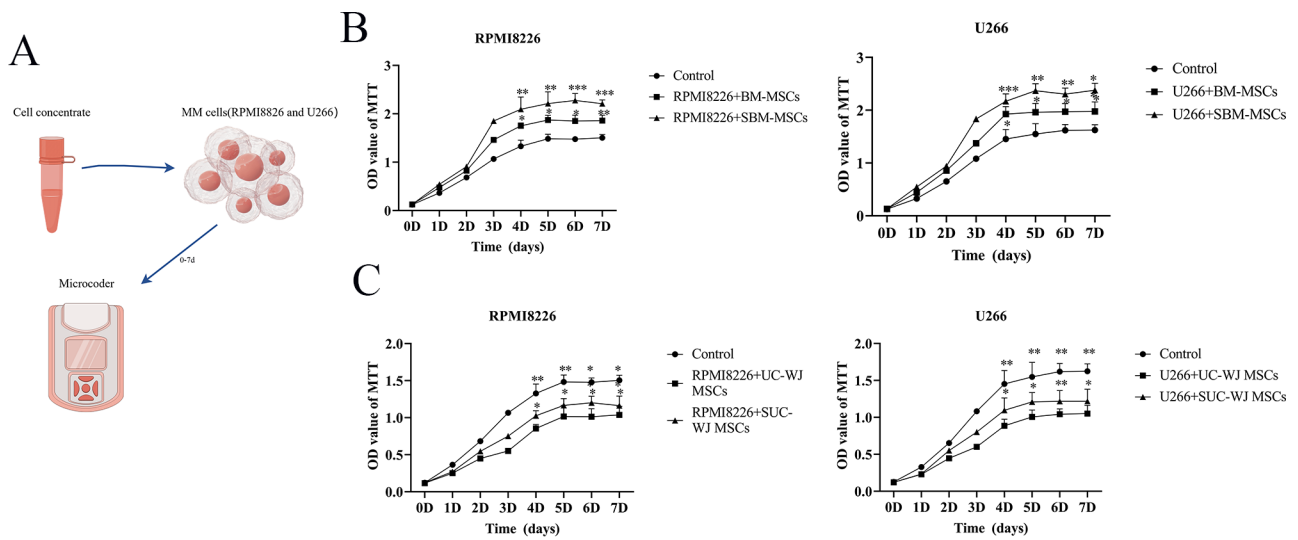


Fig. 4 The effects of concentrated supernatants from MSCs on MM cell proliferation. **(A)** Schema of experiment design: MTT assay was used to detect the proliferation of MM cells after adding different MSCs concentrates. **(B)** Effects of concentrated supernatants of BM-MSCs and SBM-MSCs on MM cells. **(C)** Effects of concentrated supernatants of UC-WJ MSCs and SUC-WJ MSCs on MM cells. * $P < 0.05$, ** $P < 0.01$ comparison with the control group

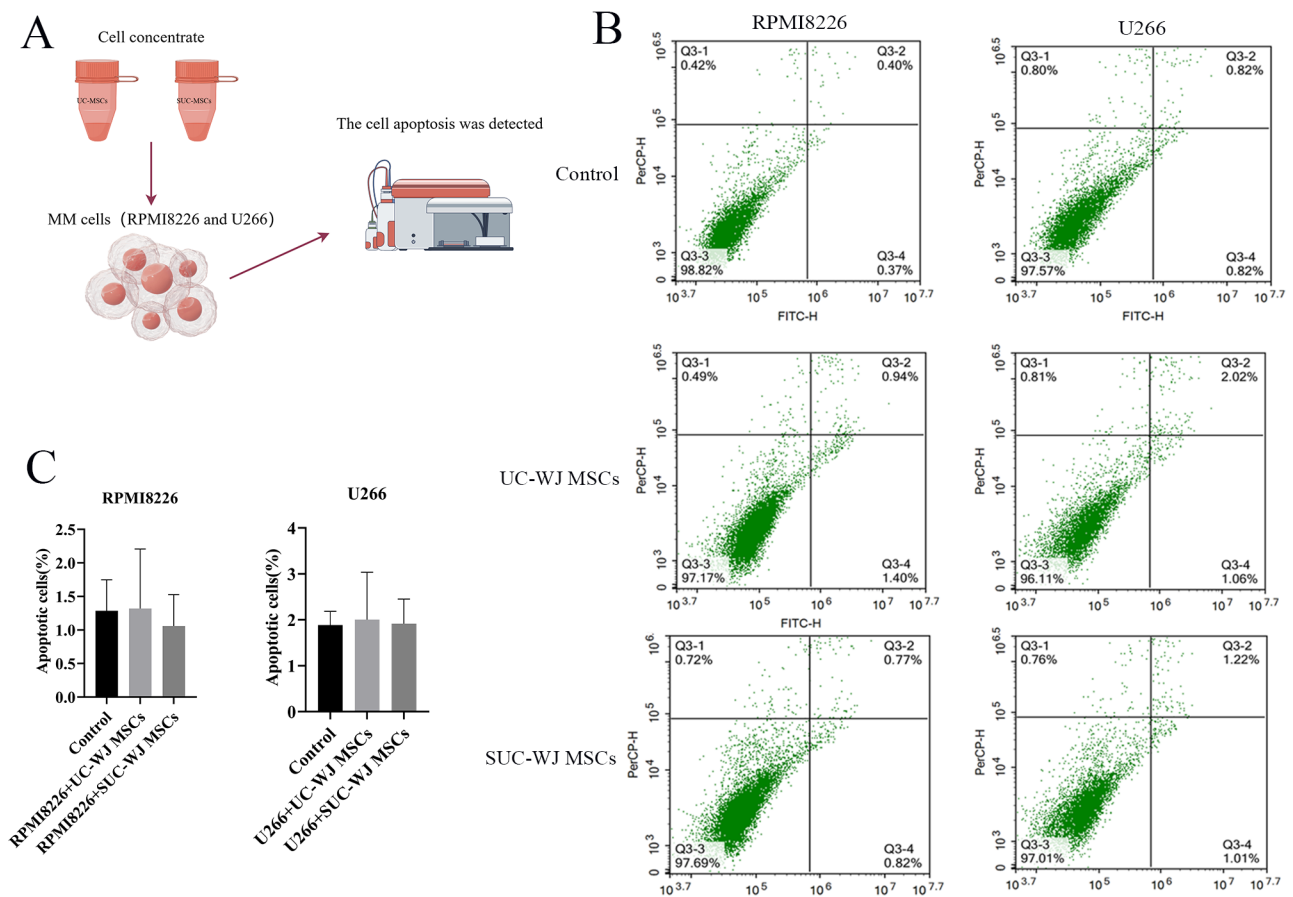


Fig. 5 Effects of UC-WJ MSCs and senescent UC-WJ MSCs (SUC-WJ MSCs) concentrated supernatants on MM cells apoptosis. **(A)** Schema of experiment design: Apoptosis of UC-WJ MSCs and SUC-WJ MSCs after the addition of MM cells by flow cytometry. **(B)** Flow cytometry was used to detect MM cells apoptosis. **(C)** Statistical analysis of MSCs concentrate added to MM cells. * $P < 0.05$, ** $P < 0.01$ comparison with the control group

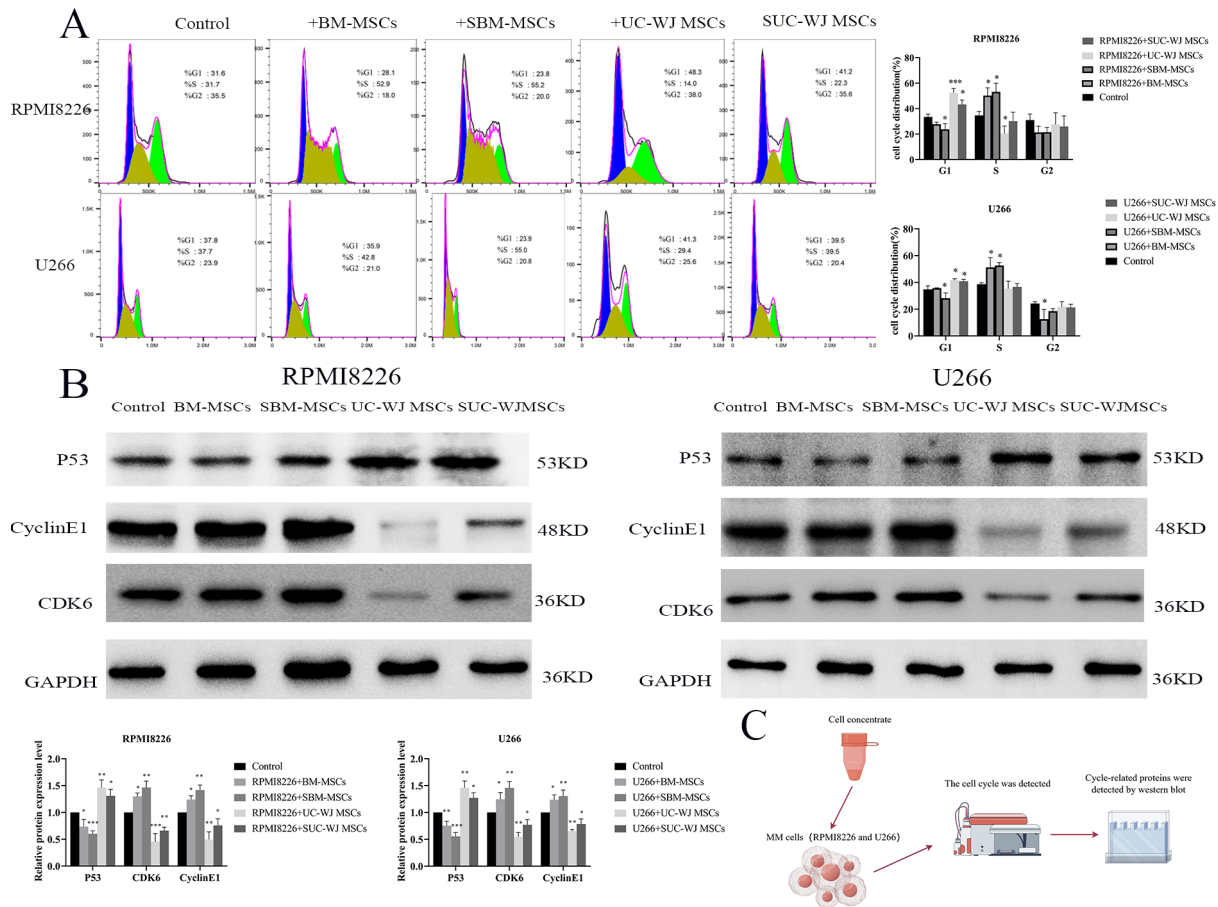


Fig. 6 Effect of MSCs supernatants on the MM cells cycle and selected protein levels. **(A)** Schema of experiment design: The effects of BM-MSCs and UC-WJ MSCs supernatants on the cell cycle of RPMI8226 and U266 cells. **(B)** Levels of CDK6, P53 and CyclinE1 in MM cells after treatment with concentrated supernatants of MSCs. **(C)** Flowchart of the process of detecting intracellular cycle changes after the incorporation of different MSCs concentrates into MM cells. * $P < 0.05$, ** $P < 0.01$, *** $P < 0.005$ comparison with the control group. Full-length gels/blots are shown in Figure S2 in the Supplementary material

the BM-MSCs supernatant (Fig. 8A). MSCs concentrate expression of tumour stemness factors after addition of MM cells (Fig. 8B).

Effects of different MSCs on soluble factor levels in MM cells

We used public databases to analyse the effects of interleukin 6 (IL-6) and vascular endothelial growth factor A (VEGFA) on the survival and prognosis of MM patients as well as the difference in expression between MM patients and healthy individuals (Fig. 9A). We observed that low expression levels of IL-6 and VEGFA were associated with prolonged survival of patients. The levels of these proteins was then detected in MM cells treated with the various MSCs supernatants using western blotting (Fig. 9B). In comparison with the control group, BM-MSCs and SBM-MSCs supernatants increased the levels of IL-6, and VEGFA proteins, with the SBM-MSCs supernatant having a more obvious effect. However, the levels of IL-6 and VEGFA were decreased by treatment with UC-WJ MSCs and SUC-WJ MSCs supernatants,

and the inhibitory effect of the UC-WJ MSCs supernatant was stronger (Fig. 9B). We analyzed the effects of interleukin 6 (IL-6) and vascular endothelial growth factor A (VEGFA) on the survival and prognosis of patients with MM using a public database (Fig. 9C), results displayed: IL6 (COX $p = 0.35$, HR = 1.08, 95%CI, 0.92 to 1.27, VEGFA (COX $p = 0.03$, HR = 1.35, 95%CI, 1.03 to 1.77). In addition, we analysed the differences in IL-6 and VEGFA expression between MM patients and healthy subjects by using the GEO database(Fig. 9D).

MSCs affected MM cells via PI3K/AKT/NF- κ B signaling

As shown in Fig. 10A, compared with the control group, UC-WJ MSCs and SUC-WJ MSCs supernatants down-regulated the levels NF- κ B, P-AKT, and P-PI3K in RPMI8226 and U266 cells, while BM-MSCs and SBM-MSCs increased NF- κ B, P-AKT, and P-PI3K levels in RPMI8226 and U266 cells. The western blotting results showed that the effects of MSCs supernatants on the biological functions of MM cells is related to PI3K/AKT/NF- κ B signaling. Chart of possible mechanisms after

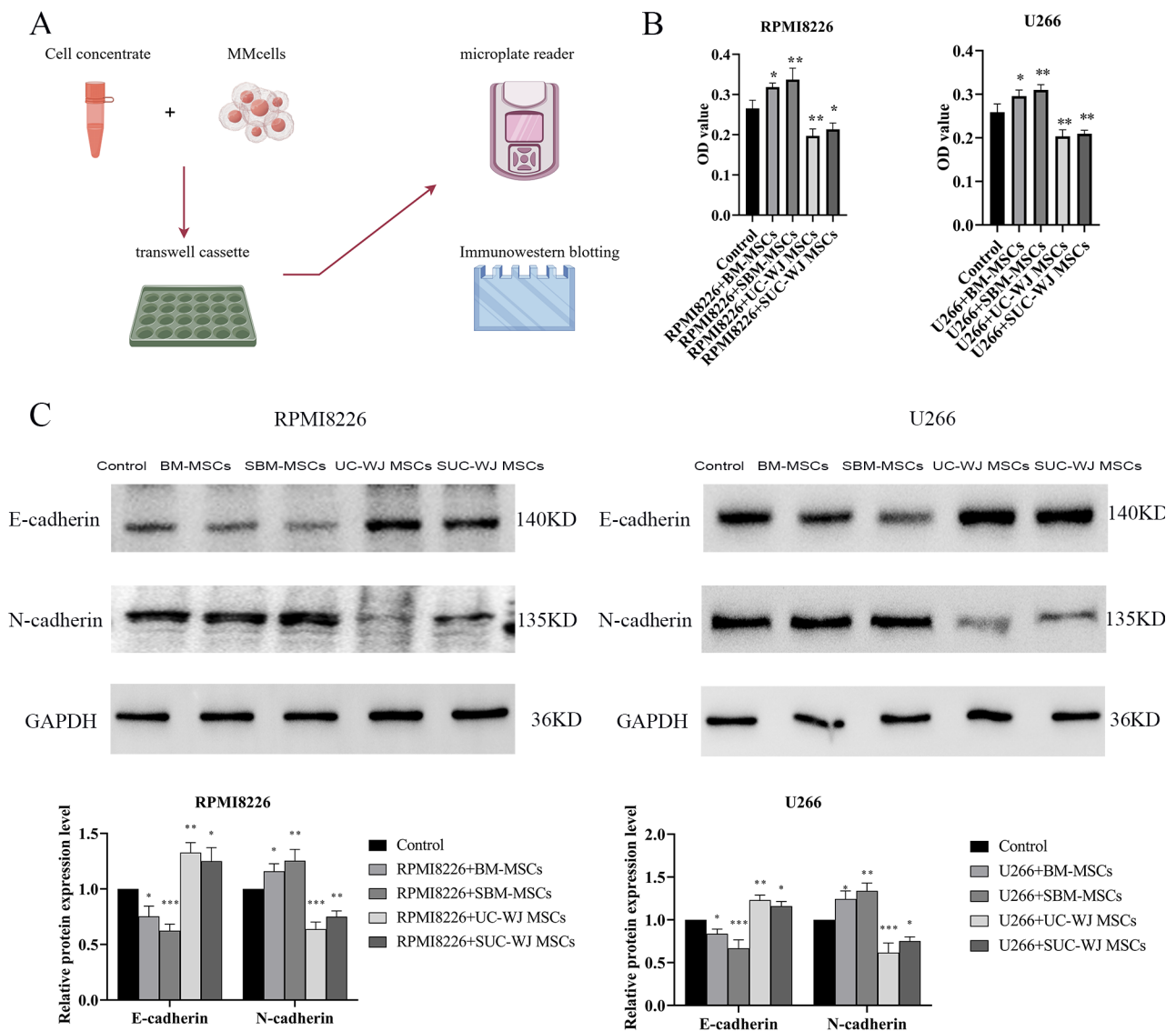


Fig. 7 Effects of MSCs concentrated supernatants on the migration of MM cells and the levels of EMT-related proteins. **(A)** Schema of experiment design: The invasive capacity was assayed after MM cells treated with different MSC concentrate supernatants. **(B)** Cell migration of MM cells treated with different MSCs concentrated supernatants. **(C)** The levels of EMT-related proteins in MM cells treated with different MSCs concentrated supernatants. * $P < 0.05$, ** $P < 0.01$, *** $P < 0.001$, comparison with the control group. Full-length gels/blots are shown in Figure S3 in the Supplementary material

addition of different MSCs concentrates to MM cells (Fig. 10B).

Discussion

MSCs, as new anti-cancer cell therapies, are currently under intensive investigation. These cells might be ideal candidates for cell therapy and tissue engineering, because of their natural homing properties to tumors and their potential as cellular carriers for targeted delivery or local production of tumor cytotoxic molecules [13, 14]. Multiple myeloma is a malignant hematological tumor that is difficult to cure [15]. It was found that BM-MSCs can promote proliferation of MM cells [16],

while UC-MSCs can inhibit proliferation of MM cells [17]. Moreover, Abnormal plasma cell can induce MSCs to exhibit senescent phenotype in MM microenvironment [18]. Herein, we investigated the potential biological function of MSCs from healthy adult bone marrow and neonatal umbilical cord tissue, as well as the effects of the concentrated supernatants from senescent MSCs induced by hydrogen peroxide on MM cells. So, the effects of different sources and states of MSCs on MM proliferation were evaluated in a unified experimental system, then the best cancer gene therapy vector was selected for MM patients.

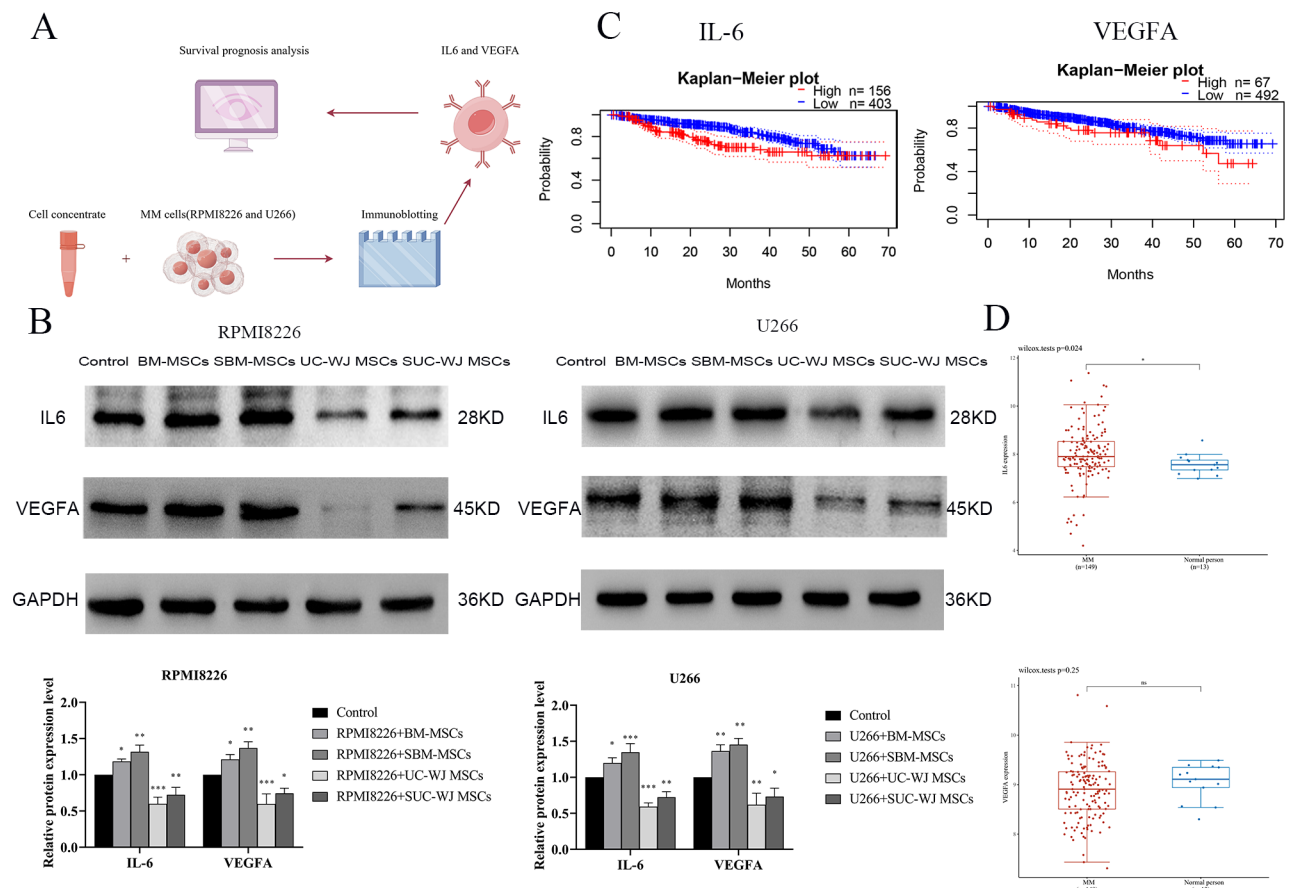


Fig. 9 MSCs supernatant concentrates affect the biological functions of RPMI8226 and U266 cells through IL-6 and VEGFA. **(A)** Schema of experiment design: To evaluate the effects of IL-6 and VEGFA on MM patients and the expression of MSCs concentrate added to MM cells. **(B)** Analysis of survival related to IL-6 and VEGFA levels in MM patients. **(C)** The levels of different MSCs concentrates on the IL-6 and VEGFA in MM cells. **(D)** Expressional differences of IL-6 and VEGFA between MM patients and healthy subjects, * $P < 0.05$, ** $P < 0.01$, *** $P < 0.001$, comparison with the control group. Full-length gels/blots are shown in Figure S5 in the Supplementary material

hallmarks of SASP are upregulated secretion of extracellular matrix remodeling factors, pro-angiogenic factors, growth factors, and in particular, pro-inflammatory cytokines (e.g., IL-8, IL-6, and IL-1 β) [28, 29]. Systemic cytokines are vital for MM clone growth and survival [30], and BM-MSCs in the MM ecotone secrete a large number of cytokines that maintain pro-tumor conditions, regulate cancer cell growth and survival, and maintain the cytokine feedback loop [31–33]. High expression of the inflammatory factor IL-6 [34, 35], the angiogenic factor VEGFA [36] are important mediators that promote MM activity and correlate negatively with patient survival [37, 38]. The BMME in MM contains high-levels of cytokines such as IL-6 and VEGF, which act as growth factors for MM cells and promote cell adhesion, thus playing a crucial role in MM development [39]. The elevated VEGF level in MM further stimulates PCs to activate IL-6 secretion, which accelerates the progression of MM [40], while overexpression VEGF and IL-6 mainly activate the PI3K signaling pathway, participating in the proliferation and

migration of MM cells [41]. The present study aimed to evaluate the effects of cytokines produced by MSCs from two sources, human bone marrow and umbilical cord, as well as their respective SMSCs cell supernatants, on MM cells. We found that supernatants from both types of MSCs induced IL-6 and VEGF and thus affected MM cell growth; however, the results were not consistent. BM-MSCs and SBM-MSCs supernatants promoted the secretion of these cytokines and thus increased MM cell proliferation, whereas UC-WJ MSCs and SUC-WJ MSCs supernatants inhibited of cytokine secretion and reduced the proliferation of MM cells.

The PI3K/AKT pathway is considered one of the major pathways that control the development of MM [42], and activation of the PI3K/AKT pathway can affect the NF κ B pathway, which is also a recognized therapeutic target in MM [43]. The PI3K/AKT/NF κ B axis downregulates E-cadherin expression, which increases tumor metastasis and invasiveness, leading to drug resistance, and increased tumor cell proliferation by regulating target

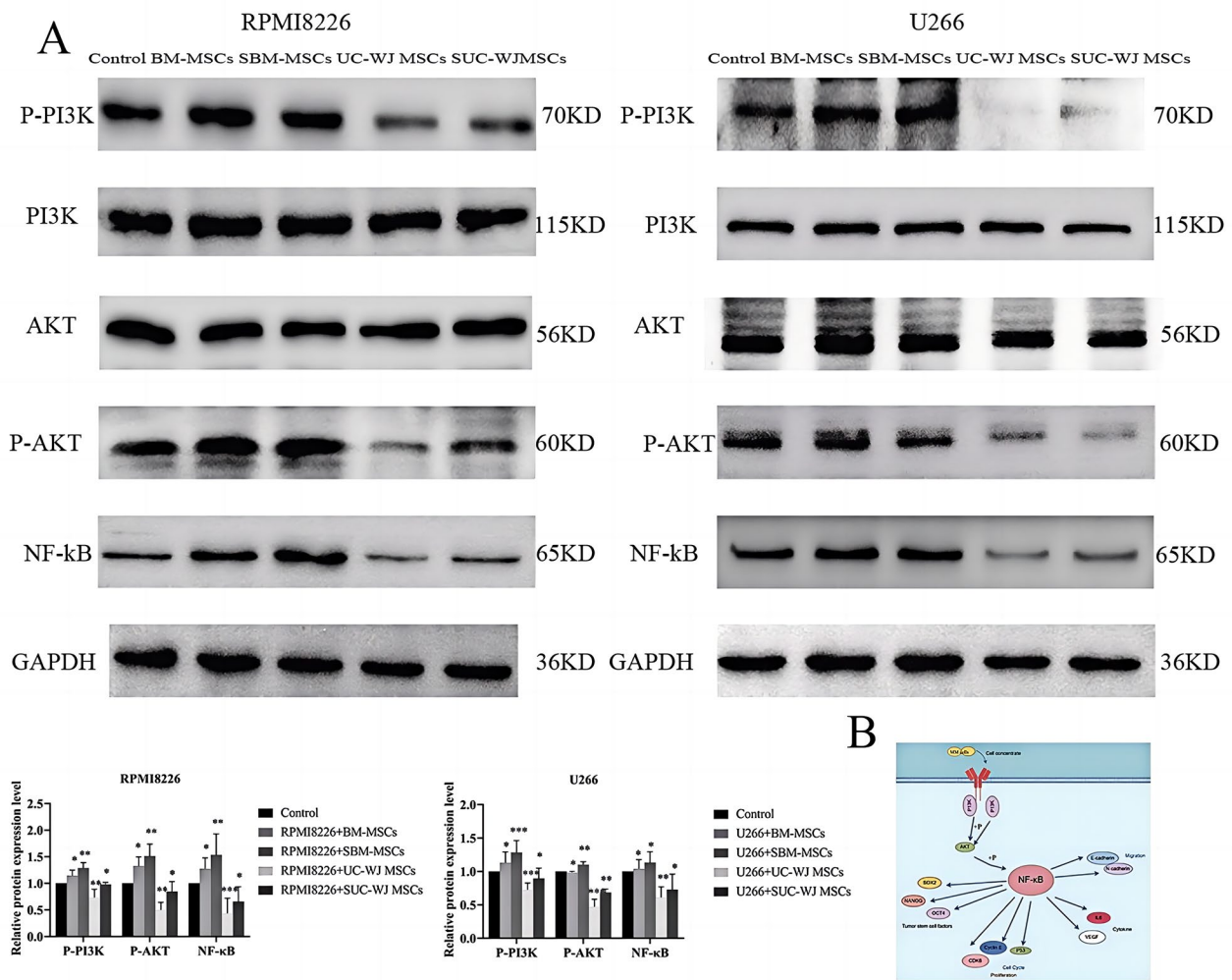


Fig. 10 MSCs superserum concentrate influences the biological function of RPMI8226 and U266 cells through PI3K/AKT/NF-κB signaling. (A) The effects of different MSCs supernatant concentrates on RPMI8226 and U266 cells are regulated, at least in part, by PI3K/AKT/NF-κB signaling. (B) Schema of experiment design: Diagram of possible mechanisms of the PI3K/AKT/NF-κB pathway after addition of MSCs concentrates to MM cells, * $P < 0.05$, ** $P < 0.01$, *** $P < 0.001$, comparison with the control group. Full-length gel/blot see supplementary Figure S6

genes and inhibiting tumor cell apoptosis [44]. Research has shown that MSCs might influence the malignant characteristics of MM cells via their effects on PI3K/AKT/NF-κB signaling [45]. This pathway is involved in the EMT and cell invasion, and EMT is also an important determinant in the metastasis of MM cells [46]. The results of the present study showed that BM-MSCs supernatants can activate PI3K/AKT/NF-κB signaling, promote MM cell migration and proliferation, and prevent MM cell apoptosis. UC-WJ MSCs supernatants were shown to have the opposite effects. Our results proved that the supernatants of UC-WJ MSCs and SUC-WJ MSCs inhibited PI3K/AKT/NF-κB signaling pathway by paracrine.

Conclusions

Our study found that UC-WJ MSCs can be used as a vector for MM gene therapy even if the multiple myeloma microenvironment has the ability to induce UC-WJ MSCs to SASP. UC-WJ MSCs and SUCMSCs can inhibit MM cells proliferation and tumor stemness factor expression by its paracrine function, These effects are closely related to inhibition of IL-6 and VEGFA secretion and down-regulation of PPI3K/AKT/NF-κB pathway.

Supplementary Information

The online version contains supplementary material available at <https://doi.org/10.1186/s13287-025-04222-8>.

Supplementary Material 1

Acknowledgements

These mechanism diagrams appeared in the paper by Figdraw.

Author contributions

LY, WFQ, LYJ, and YX conceived and designed the study. They had full access to all data in the study, and take responsibility for the integrity of the data, the accuracy of the data analysis, and the writing of the report. XX, LGY and HZX critically revised the report. CJY, CJ, YXS, and YB performed the statistical analyses. All the authors contributed to the data acquisition and analyses. All the authors have reviewed and approved the final version of the manuscript.

Funding

This work was supported by the National Natural Science Foundation of China (Nos. 82160519, 31660326, 32270848, U23A20498); the Natural Science Foundation of Guizhou Province (Nos. QianKeHe Support [2022]181, QianKeHe Basics - ZK[2023] Key 042, Qiankehe Cooperation Platform talents [2021] Postdoctoral Station 007); the Research Project of Education Department of Guizhou Province (No. QianJiaoJi [2023]037); and the Subject Excellent Reserve Talent Project (No. gyfyxkr-2023-14). The funders of the study had no role in study design, data collection, data analysis, data interpretation, or writing of the report.

Data availability

The original contributions presented in the study are included in the article/Supplementary Material. Further inquiries can be directed to the corresponding author.

Declarations

Ethics approval and consent to participate

Title of the research approval project: Mechanism study of the effect of mesenchymal stem cells in different source states on multiple myeloma, approved by the Medical Ethics Committee of the Affiliated Hospital of Guizhou Medical University, approval number: 2023 Lun Review No. (507), approval time is June 15, 2023. In this study a total of five donors, donors signed informed consent between July 2023 and May 2024. The original source has confirmed that there was initial ethical approval for collection of human cells, and that the donors had signed informed consent.

Consent for publication

All the authors contributed to the data acquisition and analyses. All the authors have reviewed and approved of the final version of the manuscript and consent to publish.

Conflict of interest

The authors have no conflicts of interest to declare.

Author details

¹Department of Hematology, The Affiliated Hospital of Guizhou Medical University, Guiyang, Guizhou Province 550001, China

²Clinical Medical Research Center, The First Affiliated Hospital of Guizhou University of Traditional Chinese Medicine, No. 71 Bao Shan North Road, Yunyan District, Guiyang, Guizhou Province 550001, China

³Third Medical Center, Chinese People's Liberation Army General Hospital, Beijing City 100039, China

⁴Key Laboratory of Adult Stem Cell Translational Research, Chinese Academy of Medical Sciences, Guizhou Medical University, No. 4 Beijing Road, Yunyan District, Guiyang, Guizhou Province 550004, China

⁵Academy of Medical Engineering and Translational Medicine, Tianjin University, Tianjin City 300072, China

Received: 14 August 2024 / Accepted: 11 February 2025

Published online: 25 February 2025

References

1. Song Y, Hejing Liu, Shuya Pan, et al. Emerging role of mesenchymal stromal cells in gynecologic cancer therapy. *Stem Cell Res Ther.* 2023;14(1):347. <https://doi.org/10.1186/s13287-023-03585-0>.
2. Ghaidaa Raheem Lateef Al-Awsi, Fahad Alsaikhan, Ria Margiana, et al. Shining the light on mesenchymal stem cell-derived exosomes. *Breast cancer Stem Cell Res Ther.* 2023;14(1):21. <https://doi.org/10.1186/s13287-023-03245-3>.
3. Yuan Ding C, Wang Z, Sun, Mesenchymal stem cells Engineered by Nonviral vectors: a powerful Tool in Cancer Gene Therapy. *Pharmaceutics.* 2021;13(6):913. <https://doi.org/10.3390/pharmaceutics13060913>
4. [4] Ursula Altanerova, Jana Jakubecova, Katarina Benejova, et al. Intracellular prodrug gene therapy for cancer mediated by tumor cell suicide gene exosomes. *Int J Cancer.* 2021;148(1):128–39. <https://doi.org/10.1002/ijc.33188>.
5. Guo Y, Zhai Y, Wu L, et al. Mesenchymal stem cell-derived extracellular vesicles: pleiotropic impacts on breast Cancer occurrence, Development and Therapy. *Int J Mol Sci.* 2022;23(6):2927. <https://doi.org/10.3390/ijms23062927>.
6. Gu J, Wang M, Wang X, et al. Exosomal mir-483-5p in bone marrow mesenchymal stem cells promotes malignant progression of multiple myeloma by targeting TIMP2. *Front Cell Dev Biol.* 2022;10:862524. <https://doi.org/10.3389/fcell.2022.862524>.
7. Ciavarella S, Caselli A, Tamma AV, et al. A peculiar molecular profile of umbilical cord-mesenchymal stromal cells drives their inhibitory effects on multiple myeloma cell growth and tumor progression. *Stem Cells Dev.* 2015;24(12):1457–70. 10.1089/scd.2014.0254.
8. Natalya Plakhova, Vasilios Panagopoulos, Kate Vandyke. Mesenchymal stromal cell senescence in haematological malignancies. *Cancer Metastasis Rev.* 2023;42(1):277–96. <https://doi.org/10.1007/s10555-022-10069-9>.
9. Juan Guo Y, Zhao C, Fei, et al. Dicer1 downregulation by multiple myeloma cells promotes the senescence and tumor-supporting capacity and decreases the differentiation potential of mesenchymal stem cells. *Cell Death Dis.* 2018;9(5):512. <https://doi.org/10.1038/s41419-018-0545-6>.
10. Mojsilović S, Jauković A, Kukulj T, et al. Tumorigenic aspects of MSC Senescence-Implication in Cancer Development and Therapy. *J Pers Med.* 2021;11(11):1133. <https://doi.org/10.3390/jpm11111133>.
11. Luo H, Pan C, Wang L, et al. Low TYROBP expression predicts poor prognosis in multiple myeloma. *Cancer Cell Int.* 2024;24(1):117. <https://doi.org/10.1186/s12935-024-03304-6>. PMID: 38549127; PMCID: PMC10979612.
12. Li Y, Yang X, Wang F, et al. Mechanism of action of Asparagus officinalis extract against multiple myeloma using bioinformatics tools, in silico and in vitro study. *Front Pharmacol.* 2023;14:1076815. <https://doi.org/10.3389/fphar.2023.1076815>. PMID: 37229244; PMCID: PMC10203399.
13. Khakoo AY, Pati S, Anderson SA, et al. Human mesenchymal stem cells exert potent antitumorigenic effects in a model of Kaposi's sarcoma. *J Exp Med.* 2006;203(5):1235–47. <https://doi.org/10.1084/jem.20051921>.
14. Xie Y, Chen F, Jia L, et al. Mesenchymal stem cells from different sources show distinct therapeutic effects in hyperoxia-induced bronchopulmonary dysplasia in rats. *J Cell Mol Med.* 2021;25(17):8558–66. <https://doi.org/10.1111/jcmm.16817>.
15. Dimopoulos MA, Jakubowiak AJ, McCarthy PL, et al. Developments in continuous therapy and maintenance treatment approaches for patients with newly diagnosed multiple myeloma. *Blood Cancer J.* 2020;10(2):17. <https://doi.org/10.1038/s41408-020-0273-x>. Published 2020 Feb 13.
16. Kawano Y, Moschetta M, Manier S, et al. Targeting the bone marrow microenvironment in multiple myeloma. *Immunol Rev.* 2015;263(1):160–72. <https://doi.org/10.1111/imr.12233>.
17. Paola Cafforio L, Viggiano F, Mannavola, et al. pIL-6-TRAIL-engineered umbilical cord mesenchymal/stromal stem cells are highly cytotoxic for myeloma cells both in vitro and in vivo. *Stem Cell Res Ther.* 2017;8(1):206. <https://doi.org/10.1186/s13287-017-0655-6>.
18. Chiara Valsecchi S, Croce A, Maltese et al. Bone marrow microenvironment in Light-Chain amyloidosis: in Vitro Expansion and characterization of mesenchymal stromal cell. *Biomedicines.* 2021;9(11):1523. 10.3390
19. Lee B, Sandhu S, McArthur G. Cell cycle control as a promising target in melanoma. *Curr Opin Oncol.* 2015;27(2):141–50. 10.1097.
20. Borgs L, Beukelaers P, Vandenbosch R, et al. Cell circadian cycle: new role for mammalian core clock genes. *Cell Cycle.* 2009;8(6):832–7. <https://doi.org/10.4161/cc.8.6.7869>.
21. Wood DJ, Endicott JA. Structural insights into the functional diversity of the CDK-cyclin family. *Open Biol.* 2018;8(9):180112. <https://doi.org/10.1098/rsob.180112>.
22. Bellutti F, Tigan AS, Nebenfuhr S, et al. CDK6 antagonizes p53-Induced responses during Tumorigenesis. *Cancer Discov.* 2018;8(7):884–97. <https://doi.org/10.1158/2159-8290>.
23. Tanno T, Lim Y, Wang Q, et al. Growth differentiating factor 15 enhances the tumor-initiating and self-renewal potential of multiple myeloma cells. *Blood.* 2014;123(5):725–33. <https://doi.org/10.1182/blood-2013-08-524025>.

24. Ilona Kaszak O, Witkowska-Piłaszewicz Z, Niewiadomska, et al. Role of cadherins in Cancer-A Review. *Int J Mol Sci.* 2020;21(20):7624. <https://doi.org/10.3390/ijms21207624>.
25. Serrano-Gomez SJ, Maziveyi M, Alahari SK. Regulation of epithelial-mesenchymal transition through epigenetic and post-translational modifications. *Mol Cancer.* 2016;15:18. <https://doi.org/10.1186/s12943-016-0502-x>.
26. Li X, Luo X, He Y, et al. Micronano titanium accelerates mesenchymal stem cells aging through the activation of senescence-associated secretory. Phenotype ACS Nano. 2023;17(22):22885–900. <https://doi.org/10.1021/acsnano.3c07807>.
27. Dominici M, Le Blanc K, Mueller I, et al. Minimal criteria for defining multipotent mesenchymal stromal cells. *Int Soc Cell Therapy Position Statement Cytotherapy.* 2006;8(4):315–7. <https://doi.org/10.1080/14653240600855905>.
28. Lee BC, Yu K. R. Impact of mesenchymal stem cell senescence on inflammaging. *BMB Rep.* 2020;53:65–73. <https://doi.org/10.5483/BMBRep.2020.53.2.291>.
29. Gnani D, Crippa S, Della Volpe L, et al. An early-senescence state in aged mesenchymal stromal cells contributes to hematopoietic stem and progenitor cell clonogenic impairment through the activation of a pro-inflammatory program. *Aging Cell.* 2019;18(3):e12933. <https://doi.org/10.1111/acer.12933>.
30. Kowalska M, Kaminska J, Foksiewicz M, et al. A survey of prognostic value of serum factors in multiple myeloma patients before treatment: macrophage-colony stimulating factor (M-CSF) is a powerful predictor of survival. *Med Oncol.* 2011;28(1):194–8. <https://doi.org/10.1007/s12032-009-9403-9>.
31. Zheng MM, Zhang Z, Bemis K, et al. The systemic cytokine environment is permanently altered in multiple myeloma. *PLoS ONE.* 2013;8(3):e58504. <https://doi.org/10.1371/journal.pone.0058504>.
32. Giannakoulas N, Ntanasis-Stathopoulos I, Terpos E. The role of Marrow Microenvironment in the growth and development of malignant plasma cells in multiple myeloma. *Int J Mol Sci.* 2021;22(9):4462. <https://doi.org/10.3390/ijms22094462>.
33. Daniel García-Sánchez A, González-González. Ana Alfonso-Fernández et al. Communication between bone marrow mesenchymal stem cells and multiple myeloma cells: impact on disease progression. *World J Stem Cells.* 2023;15(5):421–37. <https://doi.org/10.4252/wjsc.v15.i5.421>.
34. Shivali Jasrotia R, Gupta A, Sharma et al. Cytokine profile in multiple myeloma. *Cytokine.* 2020;136:155271. <https://doi.org/10.1016/j.cyto.2020.155271>.
35. Chong PSY, Zhou J, Lim JSL, et al. IL-6 promotes a STAT3-PRL3 Feed-forward Loop via SHP2 repression in multiple myeloma. *Cancer Res.* 2019;79(18):4679–88. <https://doi.org/10.1158/0008-5472.CAN-19-0343>.
36. Liu M, Liu H, Zhou J, et al. miR-140-5p inhibits the proliferation of multiple myeloma cells by targeting VEGFA. *Mol Med Rep.* 2021;23(1):53. <https://doi.org/10.3892/mmr.2020.11691>.
37. Botta C, Di Martino MT, Ciliberto D, et al. A gene expression inflammatory signature specifically predicts multiple myeloma evolution and patients survival. *Blood Cancer J.* 2016;6(12):e511. <https://doi.org/10.1038/bcj.2016.118>.
38. Gu J, Huang X, Zhang Y et al. Cytokine profiles in patients with newly diagnosed multiple myeloma: survival is associated with IL-6 and IL-17A levels. *Cytokine.* 2021;138:15535810.1016/j.cyto.2020.155358
39. Harmer D, Falank C, Reagan MR. Interleukin-6 interweaves the bone marrow microenvironment, bone loss, and multiple myeloma. *Front Endocrinol (Lausanne).* 2019;9:788. <https://doi.org/10.3389/fendo.2018.00788>.
40. Menu E, Kooijman R, Van Valckenborgh E, et al. Specific roles for the PI3K and the MEK-ERK pathway in IGF-1-stimulated chemotaxis, VEGF secretion and proliferation of multiple myeloma cells: study in the 5T33MM model. *Br J Cancer.* 2004;90(5):1076–83. <https://doi.org/10.1038/sj.bjc.6601613>.
41. Bellutti F, Tigan AS, Nebenfuehr S, et al. CDK6 antagonizes p53-Induced Responses during Tumorigenesis. *Cancer Discov.* 2018;8(7):884–97. <https://doi.org/10.1158/2159-8290.CD-17-0912>.
42. Heinemann L, Möllers KM, Ahmed HMM, et al. Inhibiting PI3K-AKT-mTOR signaling in multiple myeloma-Associated Mesenchymal stem cells impedes the proliferation of multiple myeloma cells. *Front Oncol.* 2022;12. <https://doi.org/10.3389/fonc.2022.874325>.
43. Bariana M, Cassella E, Rateshwar J, et al. Inhibition of NF- κ B DNA binding suppresses Myeloma Growth via Intracellular Redox and Tumor Microenvironment Modulation. *Mol Cancer Ther.* 2022;21(12):1798–809. <https://www.doi.org/10.1158/1535-7163.MCT-22-0257>.
44. Ranjani S, Kowshik J, Sophia J, et al. Activation of PI3K/Akt/NF- κ B signaling mediates Swedish Snus Induced Proliferation and apoptosis evasion in the Rat Forestomach: modulation by Blueberry. *Anticancer Agents Med Chem.* 2020;20(1):59–69. <https://doi.org/10.2174/1871520619666191024115738>.
45. Peng Y, Li F, Zhang P, et al. IGF-1 promotes multiple myeloma progression through PI3K/Akt-mediated epithelial-mesenchymal transition. *Life Sci.* 2022;249:117–503. <https://doi.org/10.1016/j.lfs.2020.117503>.
46. Babaei G, Aziz SG, Jaghi NZZ. EMT, cancer stem cells and autophagy; the three main axes of metastasis. *Biomed Pharmacother.* 2021;133:110909doi. <https://doi.org/10.1016/j.biopha.2020.110909>.

Publisher's note

Springer Nature remains neutral with regard to jurisdictional claims in published maps and institutional affiliations.